

Control Mechanism of Surface Subsidence and Overburden Movement in Backfilling Mining based on Laminated Plate Theory

Zhengzheng Cao¹, Feng Du^{2,3,4}, Ping Xu¹, Haixiao Lin¹, Yi Xue³, Yuejin Zhou³

Abstract: The backfilling mining technology is a type of high-efficiency coal mining technology that is used to address the environmental issues caused by the caving mining technology. In this paper, the mechanical model of symmetrical laminated plate representing the overburden movement caused by the backfilling mining technology is established, and the governing differential equation of the motion of the overburden is derived. The boundary conditions of the mechanical model are put forward, and the analytical solution of the overburden movement and surface subsidence is obtained. The numerical model of the overburden movement and surface subsidence, under mining with backfilling, is established by means of the FLAC3D numerical software, which aims to systematically study the influence of backfilling compactness, mining thickness, and mining depth on the overburden movement and surface subsidence in backfilling mining. When the compactness η is less than 70%, the overburden movement and surface subsidence is greater, while when η is greater than 70%, the overburden movement and surface subsidence is reduced significantly. On this basis, the control mechanism of surface subsidence and overburden movement in backfilling mining is obtained. The suitable backfilling compactness is the key to controlling surface subsidence and overburden movement in backfilling mining.

Keywords: Symmetrical laminated plate theory, surface subsidence, overburden movement, backfilling mining.

1 Introduction

Due to the high demand of coal and the large spread of urbanization, mining is seeking ways to obtain coal that is deposited under buildings, railways and bodies of water. Mining under structures can create hazards, such as overburden movement and surface subsidence, along with the need to dispose of the waste material that is typically stacked on the mine (such as coal gangue and coal ash). Backfilling mining technology is a safe

¹ School of Civil Engineering, Henan Polytechnic University, Jiaozuo 454000, China.

² School of Energy and Engineering, Henan Polytechnic University, Jiaozuo 454000, China.

³ State Key Laboratory of Coal Resources and Safe Mining, State Key Laboratory for Geomechanics & Deep Underground Engineering, China University of Mining and Technology, Xuzhou 221116, China.

⁴ Corresponding author: Feng Du. Tel.: +86 18639168883. E-mail address: dufeng@hpu.edu.cn.

and highly efficiency coal mining technique that has been developed specifically for this purpose and has already proven to be an effective practice [Qian (2010); Zhou, Guo, Cao, and Zhang (2013); Cao, Zhou, Xu, and Li (2014); Xue, Gao, and Liu (2015); U. Babuscu (2017)]. According to the mining practice, the overburden rock in backfill mining method presents continuous bending deformation, while periodic breakage of overburden rock is mainly shown in the caving mining method [Zhang, Miao, and Guo (2009); Miao (2012); Ding, Zhou, Xu, Peng, and Cao (2013); Ju, Li, Zhang, Miao, and Liu (2014); Zhou, Tian, and Zhang (2016)]. Considering that the overburden rock behaves dramatically differently during backfill mining method than during the caving mining method, in-depth research needs to be conducted on the overburden movement and surface subsidence mechanisms under backfill mining and a corresponding strata control theory of backfill mining needs to be established [Pankow, Waas, and Yen (2012); Miao, Wei, and Yan (2013); Xie, Xu, Wang, Guo, and Liu (2014); Xin and Ji (2016)].

Currently, the research on strata control under backfill mining mainly focuses on the mechanical model of a rock beam, which describes the central region of the working face reasonably [Qian, Miao, and Xu (2008); Zhang, Li, and An (2010); Miao, Huang, and Ju (2012); Ning, Wang, Liu, Qian, and Sun (2014); Jia, Qiao, and Jiang (2016)]. As this rock beam model attribute the movement of overburden rock to the plane strain type, the deformation of the edge of the working face cannot be illustrated properly [Miao, Zhang, and Guo (2010); Zhou, Chen, Zhang, and He (2012); Cao and Zhou (2015); Yi and Cui (2015); Xue, Ranjith, Gao, Zhang, Cheng, Chong, and Hou (2017)]. Therefore, based on the deformation characteristics of overburden rock under backfill mining, the mechanical model of a symmetrical laminated plate is adopted in this paper, which is beneficial to an in-depth analysis of the deformation of the overburden strata under backfill mining.

2 Mechanical analysis of overburden movement under backfill mining

The fully mechanized mining with solid backfilling consists of five key production systems, namely the coal transport system, auxiliary transport system, ventilation system, solid waste transport system, and a backfill system. The coal transport system, auxiliary transport system, and ventilation system are the same as those used in traditional fully mechanized coal mining. The solid waste transport system transports the solid waste from the surface to the underground working face, and the backfill system places the dense backfill material in the gob area, which is developed to handle solid backfill materials as an integral part of the original fully mechanized coal mining system.

As continuous slight-bending deformation of overburden strata is produced under backfill mining, the overburden strata structure is simplified into a symmetrical laminated plate structure consisting of several isotropic strata based upon the hierarchical structure and soft-hard alternating characteristics of overburden strata.

When the working face is advanced under backfill mining, concurrent deformation of overburden strata occurs, the deflection expression in various strata become consistent, and combined with the deflection expression in plate theory [Xu (2005)]:

$$w = \frac{16q_0}{\pi^6 D} \sum_{m=1,3,5,\dots}^{\infty} \sum_{n=1,3,5,\dots}^{\infty} \frac{\sin(m\pi x/a) \sin(n\pi y/b)}{mn(m^2/a^2 + n^2/b^2)^2} \quad (1)$$

The q_0 is the topsoil load, and the coefficients (a, b) in various strata are consistent. And combined with the bending rigidity, the expression of curvature and torsion rate in plate theory [Xu (2005)], Therefore:

$$\left\{ \begin{array}{l} \frac{M_x^1(1-\mu_1^2)}{E_1 h_1^3 (\chi_x^1 + \mu_1 \chi_y^1)} = \frac{M_x^2(1-\mu_2^2)}{E_2 h_2^3 (\chi_x^2 + \mu_2 \chi_y^2)} = \dots = \frac{M_x^i(1-\mu_i^2)}{E_i h_i^3 (\chi_x^i + \mu_i \chi_y^i)} = \dots = \frac{M_x^n(1-\mu_n^2)}{E_n h_n^3 (\chi_x^n + \mu_n \chi_y^n)} \\ \frac{M_y^1(1-\mu_1^2)}{E_1 h_1^3 (\chi_y^1 + \mu_1 \chi_x^1)} = \frac{M_y^2(1-\mu_2^2)}{E_2 h_2^3 (\chi_y^2 + \mu_2 \chi_x^2)} = \dots = \frac{M_y^i(1-\mu_i^2)}{E_i h_i^3 (\chi_y^i + \mu_i \chi_x^i)} = \dots = \frac{M_y^n(1-\mu_n^2)}{E_n h_n^3 (\chi_y^n + \mu_n \chi_x^n)} \\ \frac{M_{xy}^1(1+\mu_1)}{G_1 h_1^3 \chi_{xy}^1} = \frac{M_{xy}^2(1+\mu_2)}{G_2 h_2^3 \chi_{xy}^2} = \dots = \frac{M_{xy}^i(1+\mu_i)}{G_i h_i^3 \chi_{xy}^i} = \dots = \frac{M_{xy}^n(1+\mu_n)}{G_n h_n^3 \chi_{xy}^n} \end{array} \right. \quad (2)$$

The overburden movement could be controlled effectively through the backfilling mining technology [Miao, Huang, and Ju (2012)]. Namely, the curvature rate (χ_x, χ_y) in overburden strata could be regarded as the tiny value. The rate of curvature and torsion in various strata become consistent under backfill mining, therefore:

$$\left\{ \begin{array}{l} \frac{M_x^1(1-\mu_1^2)}{E_1 h_1^3} = \frac{M_x^2(1-\mu_2^2)}{E_2 h_2^3} = \dots = \frac{M_x^i(1-\mu_i^2)}{E_i h_i^3} = \dots = \frac{M_x^n(1-\mu_n^2)}{E_n h_n^3} \\ \frac{M_y^1(1-\mu_1^2)}{E_1 h_1^3} = \frac{M_y^2(1-\mu_2^2)}{E_2 h_2^3} = \dots = \frac{M_y^i(1-\mu_i^2)}{E_i h_i^3} = \dots = \frac{M_y^n(1-\mu_n^2)}{E_n h_n^3} \\ \frac{M_{xy}^1(1+\mu_1)}{G_1 h_1^3} = \frac{M_{xy}^2(1+\mu_2)}{G_2 h_2^3} = \dots = \frac{M_{xy}^i(1+\mu_i)}{G_i h_i^3} = \dots = \frac{M_{xy}^n(1+\mu_n)}{G_n h_n^3} \end{array} \right. \quad (3)$$

Because the total bending moment and torque of the laminated plate structure of overburden rock are shared by each section of single rock layer, and assuming that $m_x^i, m_y^i, m_{xy}^i, m_{yx}^i$ as the moment and torque per unit length of the cross section:

$$\left\{ \begin{array}{l} m_x^i = \frac{E_i h_i^3 \sum_{k=1}^n (1-\mu_k^2)}{(1-\mu_i^2) \sum_{k=1}^n E_k h_k^3} m_x^{sum} \\ m_y^i = \frac{E_i h_i^3 \sum_{k=1}^n (1-\mu_k^2)}{(1-\mu_i^2) \sum_{k=1}^n E_k h_k^3} m_y^{sum} \\ m_{xy}^i = m_{yx}^i = \frac{G_i h_i^3 \sum_{k=1}^n (1+\mu_k)}{(1+\mu_i) \sum_{k=1}^n G_k h_k^3} m_{xy}^{sum} \end{array} \right. \quad (4)$$

Combined with the expression of the deflection w_i per unit length of the i strata in cross section [Xu (2005)]:

$$\left\{ \begin{aligned} m_x^{sum} &= -D_i \left(\frac{\partial^2 w_i}{\partial x^2} + \mu_i \frac{\partial^2 w_i}{\partial y^2} \right) \frac{(1 - \mu_i^2) \sum_{k=1}^n E_k h_k^3}{E_i h_i^3 \sum_{k=1}^n (1 - \mu_k^2)} \\ m_y^{sum} &= -D_i \left(\frac{\partial^2 w_i}{\partial y^2} + \mu_i \frac{\partial^2 w_i}{\partial x^2} \right) \frac{(1 - \mu_i^2) \sum_{k=1}^n E_k h_k^3}{E_i h_i^3 \sum_{k=1}^n (1 - \mu_k^2)} \\ m_{xy}^{sum} = m_{yx}^{sum} &= -D_i (1 - \mu_i) \frac{\partial^2 w_i}{\partial x \partial y} \frac{(1 + \mu_i) \sum_{k=1}^n G_k h_k^3}{G_i h_i^3 \sum_{k=1}^n (1 + \mu_k)} \end{aligned} \right. \quad (5)$$

Omitting the hexahedron $h \cdot dx \cdot dy$ from the symmetrical laminated plate mechanical model (Fig. 1), torque balance equations can be obtained with the torque shaft axis in parallel to the axis y and x through differential block center, respectively. Meanwhile, the force balance equation along the z axis is as follows:

$$\left\{ \begin{aligned} \sum (M)_y &= -f_{sx}^{sum} \frac{dx}{2} - (f_{sx}^{sum} + \frac{\partial f_{sx}^{sum}}{\partial x} dx) \frac{dx}{2} - m_x^{sum} + (m_x^{sum} + \frac{\partial m_x^{sum}}{\partial x} dx) - m_{yx}^{sum} + (m_{yx}^{sum} + \frac{\partial m_{yx}^{sum}}{\partial x} dx) = 0 \\ \sum (M)_x &= f_{sy}^{sum} \frac{dy}{2} + (f_{sy}^{sum} + \frac{\partial f_{sy}^{sum}}{\partial y} dy) \frac{dy}{2} + m_y^{sum} - (m_y^{sum} + \frac{\partial m_y^{sum}}{\partial y} dy) + m_{xy}^{sum} - (m_{xy}^{sum} + \frac{\partial m_{xy}^{sum}}{\partial y} dy) = 0 \\ \sum F_z &= -f_{sx}^{sum} dy + (f_{sx}^{sum} + \frac{\partial f_{sx}^{sum}}{\partial x} dx) dy - f_{sy}^{sum} dx + (f_{sy}^{sum} + \frac{\partial f_{sy}^{sum}}{\partial y} dy) dx + q dx dy = 0 \end{aligned} \right. \quad (6)$$

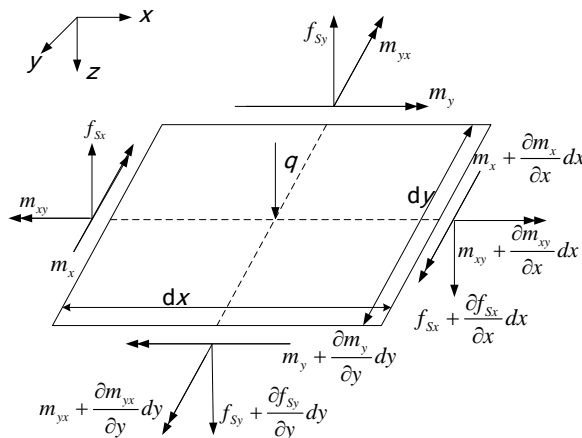


Figure 1: Mechanical model of the hexahedron

Therefore:

$$\frac{\partial^4 w_i}{\partial x^4} + 2 \left[\mu_i + 2(1 - \mu_i^2) \left(\frac{(1 + \mu_i) \sum_{k=1}^n G_k h_k^3}{(1 - \mu_i^2) \sum_{k=1}^n E_k h_k^3} \right) \right] \left[\frac{\partial^4 w_i}{\partial x^2 \partial y^2} + \frac{\partial^4 w_i}{\partial y^4} \right] = q \frac{E_i h_i^3 \sum_{k=1}^n (1 - \mu_k^2)}{D_i (1 - \mu_i^2) \sum_{k=1}^n E_k h_k^3} \quad (7)$$

If $A_i = \mu_i + 2(1 - \mu_i^2) \frac{(1 + \mu_i) \sum_{k=1}^n G_k h_k^3}{(1 - \mu_i^2) \sum_{k=1}^n E_k h_k^3}$, $B_i = \frac{(E_i h_i^3) \sum_{k=1}^n (1 - \mu_k^2)}{D_i (1 - \mu_i^2) \sum_{k=1}^n E_k h_k^3}$, the governing differential

equation of overburden movement is expressed as formula (8), based on the symmetrical laminated plate theory:

$$\frac{\partial^4 w_i}{\partial x^4} + 2A_i \frac{\partial^4 w_i}{\partial x^2 \partial y^2} + \frac{\partial^4 w_i}{\partial y^4} = qB_i \quad (8)$$

The load $q(x, y)$ is expressed as follows:

$$q(x, y) = q_0 + p = q_0 - kw \quad (9)$$

The distributed load q_0 is the topsoil load, and p is the support force by the backfill solid, which can be described by the wrinkle foundation assumption. Combining formula (8) with formula (9) gives:

$$\frac{\partial^4 w_i}{\partial x^4} + 2A_i \frac{\partial^4 w_i}{\partial x^2 \partial y^2} + \frac{\partial^4 w_i}{\partial y^4} + kB_i w_i = q_0 B_i \quad (10)$$

The boundary condition is regarded as simply supported on four sides when the burial depth of a coal seam is relatively shallow. The deflection expression is obtained:

$$w_i = \frac{16B_i q_0}{\pi^2} \sum_{m=1,3,5}^{\infty} \sum_{n=1,3,5}^{\infty} \frac{\sin(m\pi x/a) \sin(n\pi y/b)}{mn \left[\pi^4 (m^4/a^4 + 2A_i m^2 n^2/a^2 b^2 + n^4/b^4) + kB_i \right]} \quad (11)$$

The deflection w_i of the i overburden strata is expressed in formula (11), and it can be seen that the deflection w_i is hinged on q_0 (topsoil load) and k (foundation coefficient). The distributed topsoil load q_0 is proportional to the mining depth H , while the foundation coefficient k is related to the backfilling compactness η and the mining thickness h . In order to further study the influence of backfilling compactness, mining thickness and mining depth on the movement of overburden rock, the numerical method with FLAC3D numerical software is introduced.

3 Numerical simulation of overburden strata under backfill mining

3.1 Numerical calculation model

FLAC3D (Fast Lagrangian Analysis of Continua) is the finite-difference computer codes for geomechanics applications, which can simulate a full range of nonlinear static and dynamic mechanical problems. Therefore, it is suited for modeling the deformation of the overburden strata and surface subsidence controlled Backfilling mining technology. This paper establishes the numerical calculation model of strata movement under filling mining using FLAC3D numerical software as the analysis platform.

The size of the numerically calculated mechanical model is 1500m ×500m×400m, and the working face is advanced from 400 m to 1000 m with an advancing length of 600 m. The boundary conditions are set so that the bottom of the model restricts the vertical displacement and the four sides of the model restrict the horizontal displacement. The mechanical parameters of each single strata and the backfill solid are shown in Tab. 1 and Tab. 2.

Table 1: Mechanical parameters of each single strata

No.	lithology	depth /m	Density /kg m ⁻³	bulk modulus /GPa	shear modulus /GPa	tensile strength /MPa	Cohesion /MPa	internal friction angle /°
1	topsoil	135	1300	5.6	1.85	1.0	1.5	26
2	sandstone	35	2500	22.7	11.70	5.0	8.3	32
3	mudstone	40	2400	8.3	3.80	1.5	6.1	30
4	sand and mudstone	65	2300	11.4	5.80	2.0	6.5	31
5	sandstone	36	2300	15.2	7.80	5.0	6.4	31
6	mudstone	20	2400	8.3	3.80	1.0	6.1	30
7	sandstone	36	2500	16.7	10.00	5.0	8.3	32
8	coal seam	3	1800	4.2	1.09	0.5	2.1	28
9	sandstone	30	2500	16.7	10.00	5.0	8.3	32

Table 2: Mechanical parameters of the backfill solid

$\eta/\%$	50	60	70	80	90
K/GPa	0.009	0.013	0.022	0.057	0.179
G/GPa	0.006	0.007	0.013	0.022	0.030

3.2 Numerical calculation scheme

The backfilling compactness is the ratio of the mass of the backfill body backfilled into the gob to the mass of raw coal, which is regarded as a direct control indicator which

could guarantee the backfill effect. Therefore, it is important to design the backfilling compactness by considering the condition of surface structures in the mining area to guarantee that sufficient solid backfill material is used so as to control overburden movement and surface subsidence.

(1) The mining thickness is 3 m and the mining depth is 370 m. The backfilling compactness η is set to 50%, 60%, 70%, 80% and 90% in order to research the effects of backfilling compactness on the overburden movement and surface subsidence.

(2) The backfilling compactness is 80% and the mining depth is 370 m. The mining thickness h is set to 2 m, 2.5 m, 3 m, 3.5 m and 4 m in order to research the effects of mining thickness on the overburden movement and surface subsidence.

(3) The backfilling compactness is 80% and the mining thickness is 3 m. The mining depth H is set to 300 m, 350 m, 400 m, 450 m and 500 m in order to research the effects of mining depth on the overburden movement and surface subsidence.

3.3 Influence of backfilling compactness on overburden movement and surface subsidence

The sinking curve of the key strata in different backfilling compactness is shown in Fig. 2. It can be clearly seen that when the working face advances, large sinking deformation still exists when η is 50% and 60%, while the key strata only appear to have less continuous bending deformation when η is larger than 70%. When η increases from 50% to 70%, the amount of sinking that the key strata undergo reduces from 1500 mm to 690 mm, a total decrease of 810 mm.

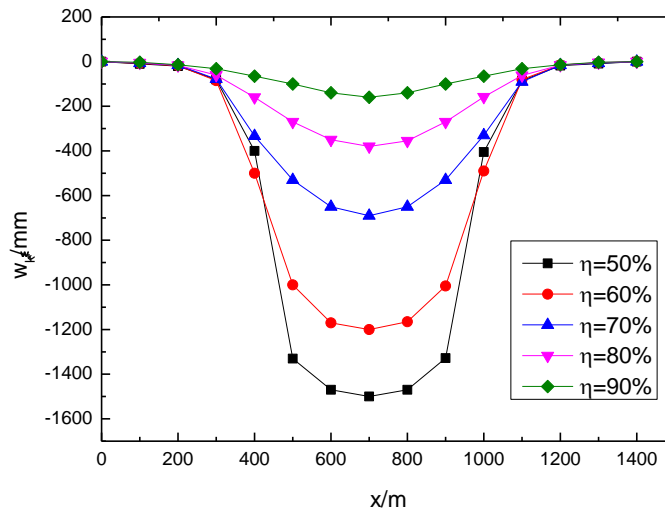


Figure 2: The sinking curve of the key strata in various backfilling compactness

The sinking curve of surface subsidence with various values of η is shown in Fig. 3. It can be observed that with an increase of η , the surface subsidence quantity decreases simultaneously. When η is larger than 70%, the surface subsidence quantity reduces significantly. For instance, when η increases from 50% to 70%, the surface subsidence

quantity reduces from 1400mm to 670 mm, a total decrease of 730 mm.

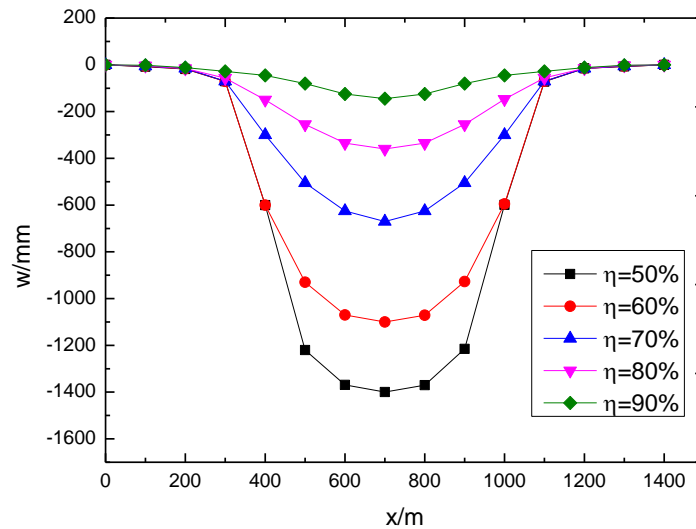


Figure 3: The sinking curve of surface subsidence in various backfilling compactness

3.4 Influence of mining thickness on overburden movement and surface subsidence

The sinking curve of the key strata in various mining thickness is shown in Fig. 4. It can be clearly seen that an approximate linear relationship is observed between mining thickness and overburden movement. When h increases from 2.0 m to 4.0 m, the amount of sinking that the key strata undergoes increases from 195 mm to 288 mm, a total increase of 93 mm.

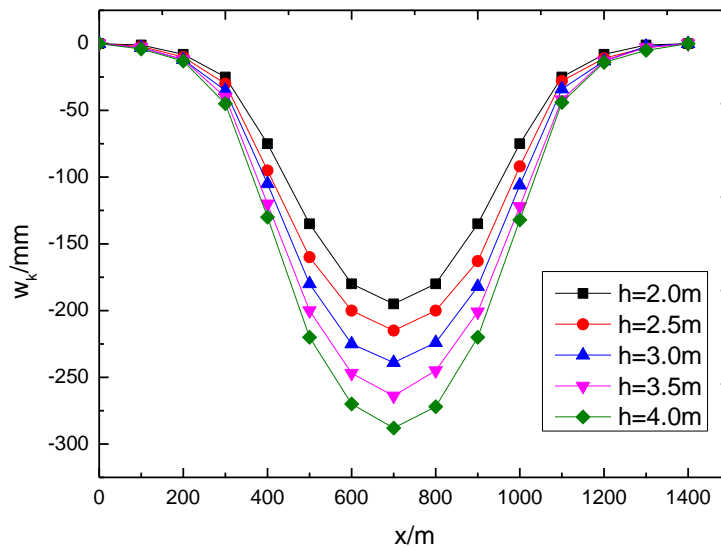


Figure 4: The sinking curve of the key strata in various mining thickness

The sinking curve of surface subsidence with various values of h is shown in Fig. 5. It can be observed that a linear relationship also exists between mining thickness and surface subsidence quantity approximately. When h increases from 2.0 m to 4.0 m, the surface subsidence quantity increases from 175 mm to 260 mm, a total increase of 85 mm.

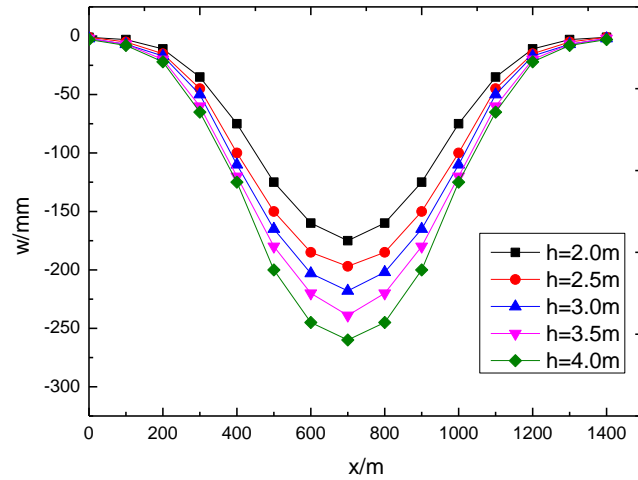


Figure 5: The sinking curve of surface subsidence in various mining thickness

3.5 Influence of mining depth on overburden movement and surface subsidence

The sinking curve of the key strata in various mining depth is shown in Fig. 6. It can be clearly seen that the overburden movement is proportional to mining depth approximately. When H increases from 300 m to 500 m, the amount of sinking that the key strata undergoes increases from 218 mm to 284 mm, a total increase of 66 mm.

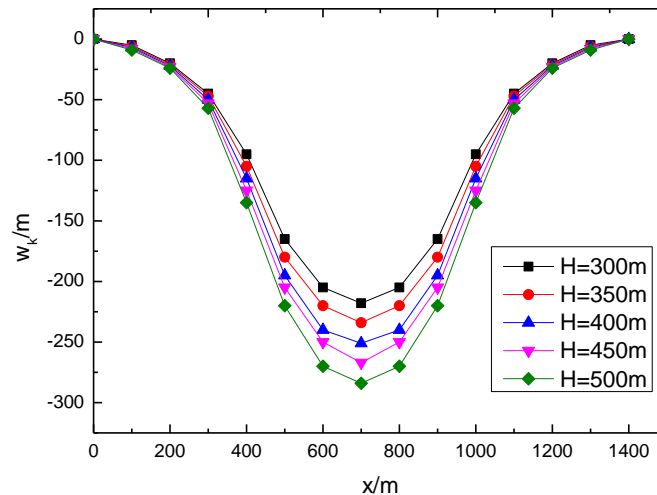


Figure 6: The sinking curve of the key strata in various mining depth

The sinking curve of surface subsidence with various values of H is shown in Fig. 7. It can be observed that the quantity of surface subsidence increases with the growth of H , and the increasing gradient of surface subsidence decreases with the increase of H . When H increases from 300 m to 500 m, the surface subsidence quantity increases from 205 mm to 232 mm, a total increase of 27 mm.

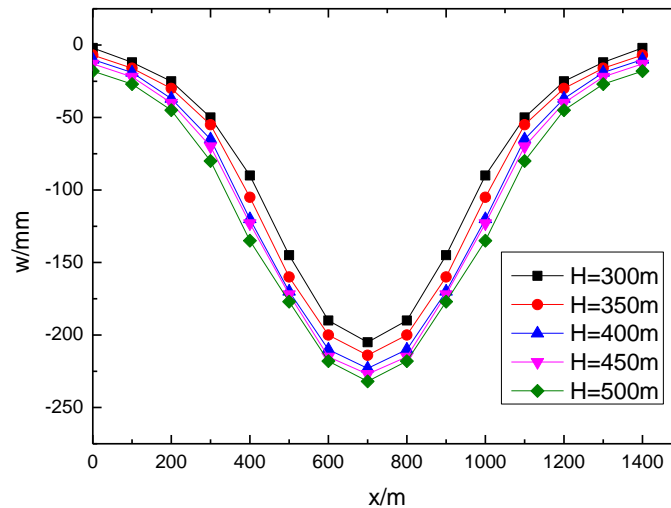


Figure 7: The sinking curve of surface subsidence in various mining depth

4 Conclusions

(1) Based on the technological principle of fully mechanized mining with solid backfilling, the symmetrical laminated plate mechanical model of overburden movement and surface subsidence is established in backfilling mining technology; on this basis, the governing differential equation of the symmetrical laminated plate mechanical model is put forward, and the analytical displacement expression of overburden strata is obtained with the definite solution condition.

(2) Simulation results indicate that the influence of backfilling compactness (η) on the sinking amount of overburden strata and surface subsidence is more significant compared with that of mining thickness and mining depth. When η is less than 70%, the sinking amount of overburden strata and surface subsidence is considerable; whereas when η is greater than 70%, the sinking quantity of overburden strata and surface subsidence is significantly reduced.

(3) The control mechanism of surface subsidence and overburden movement in solid backfilling mining is obtained. The key to controlling surface subsidence is to restrict the deformation and fracture of key strata in overburden structure. In engineering practice, the suitable solid backfilling mining scheme could be chosen by reference to the change law of key strata with backfilling compactness, thus the surface subsidence and overburden deformation is confined within the specified range.

Acknowledgement: This work was supported by the National Natural Science Foundation of China (51504081, 51704095, 51374201), the National Key Research and Development Program of China (2017YFC0805202), the Scientific Research Key Project Fund of Education Department of Henan Province (18A440012, 14A440001), the Research Fund of Henan Key Laboratory for Green and Efficient Mining and Comprehensive Utilization of Mineral Resources (S201619), the Research Fund of the State Key Laboratory of Coal Resources and Safe Mining (13KF02), the Ph.D. Programs Foundation of Henan Polytechnic University (B2014-50, B2016-67).

References

- Cao, Z. Z.; Zhou, Y. J.** (2015): Research on coal pillar width in roadway driving along goaf based on the stability of key block. *CMC: Computers Materials & Continua*, vol. 48, no. 2, pp. 77-90.
- Cao, Z. Z.; Zhou, Y. J.; Xu, P.; Li, J. W.** (2014): Mechanical response analysis and safety assessment of shallow-buried pipeline under the influence of mining. *CMES: Computer Modeling in Engineering & Sciences*, vol. 101, no. 5, pp. 351-364.
- Ding, Y. L.; Zhou, Y. J.; Xu, P.; Peng, G.; Cao, Z. Z.** (2013): Mechanism analysis of restraining surface cracks and protecting Tetraena mongolica maxin with backfilling mining. *Journal of Mining & Safety Engineering*, vol. 30, no. 6, pp. 868-873.
- Jia, H. S.; Qiao, A. Z.; Jiang, W. Y.** (2016): Deformation-failure characteristics and supporting method of mining tunnel roof in Buertai mine. *Journal of Henan Polytechnic University (Natural Science)*, vol. 35, no. 3, pp. 338-344.
- Ju, F.; Li, M.; Zhang, J. X.; Miao, X. X.; Liu, Z.** (2014): Construction and stability of an extra-large section chamber in solid backfill mining. *International Journal of Mining Science and Technology*, vol. 24, no. 6, pp. 763-768.
- Miao, C. Q.; Wei, Y. T.; Yan, X. Q.** (2013): Interactions of three parallel square-hole cracks in an infinite plate subjected to internal pressure. *CMES: Computer Modeling in Engineering & Sciences*, vol. 95, no. 6, pp. 489-504.
- Miao, X. X.** (2012): Progress of fully mechanized mining with solid backfilling technology. *Journal of China Coal Society*, vol. 37, no. 8, pp. 1247-1255.
- Miao, X. X.; Huang, Y. L.; Ju, F.** (2012): Strata movement theory of dense backfill mining. *Journal of China University of Mining & Technology*, vol. 41, no. 6, pp. 863-867.
- Miao, X. X.; Zhang, J. X.; Guo, G. L.** (2010): Study on waste-filling method and technology in fully-mechanized coal mining. *Journal of China Coal Society*, vol. 35, no. 1, pp. 1-6.
- Ning, J. G.; Wang, J.; Liu, X. S.; Qian, K.; Sun, B.** (2014): Soft-strong supporting mechanism of gob-side entry retaining in deep coal seams threatened by rockburst. *International Journal of Mining Science and Technology*, vol. 24, no. 6, pp. 805-810.
- Pankow, M.; Waas, A. M.; Yen, C. F.** (2012): Modeling the response of 3D textile composites under compressive loads to predict compressive strength. *CMC: Computers Materials & Continua*, vol. 32, no. 2, pp. 81-106.
- Qian, M. G.** (2010): On sustainable coal mining in China. *Journal of China Coal Society*,

vol. 35, no. 4, pp. 529-534.

Qian, M. G.; Miao, X. X.; Xu, J. L. (2008): On scientized mining. *Journal of Mining & Safety Engineering*, vol. 25, no. 1, pp. 1-10.

U. Babuscu, Y. (2017): Forced and natural vibrations of an orthotropic pre-stressed rectangular plate with neighboring two cylindrical cavities. *CMC: Computers Materials & Continua*, vol. 53, no. 1, pp. 1-23.

Wang, G. G.; Zhang, J. L.; Shao, J. G.; Li, K. J.; Zuo, H.B. (2015): Investigation of non-isothermal and isothermal gasification process of coal char using different kinetic model. *International Journal of Mining Science and Technology*, vol. 25, no. 1, pp. 15-21.

Xie, J. L.; Xu, J. L.; Wang, F.; Guo, J. L.; Liu, D. L. (2014): Deformation effect of lateral roof roadway in close coal seams after repeated mining. *International Journal of Mining Science and Technology*, vol. 24, no. 5, pp. 597-601.

Xin, Y. J.; Ji, H. Y. (2016): Study on uniaxial compression experiments for different ratio and large-scale similar simulated specimens. *Journal of Henan Polytechnic University (Natural Science)*, vol. 35, no. 1, pp. 30-36.

Xu, Z.L. (2005): *Elasticity*. Higher Education Press.

Xue, Y.; Gao, F.; Liu X. G. (2015): Effect of damage evolution of coal on permeability variation and analysis of gas outburst hazard with coal mining. *Natural Hazards*, vol. 79, no. 2, pp. 999-1013.

Xue, Y.; Ranjith, P. G.; Gao, F.; Zhang, D. C.; Cheng, H. M.; Chong, Z. H.; Hou, P. (2017): Mechanical behaviour and permeability evolution of gas-containing coal from unloading confining pressure tests. *Journal of Natural Gas Science and Engineering*, vol. 40, pp. 336-346.

Yi, W. X.; Cui, Y. J. (2015): Setting of waterproof coal pillar on weak water conductivity fault. *Journal of Henan Polytechnic University (Natural Science)*, vol. 34, no. 1, pp. 46-52.

Zhang, J. X.; Li, J.; An, T. L. (2010): Deformation characteristic of key stratum overburden by raw waste backfilling with fully-mechanized coal mining technology. *Journal of China Coal Society*, vol. 35, no. 3, pp. 357-362.

Zhang, J. X.; Miao, X. X.; Guo, G. L. (2009): Development status of backfilling technology using raw waste in coal mining. *Journal of Mining & Safety Engineering*, vol. 26, no. 4, pp. 395-401.

Zhou, Y. J.; Chen, Y.; Zhang, J. X.; He, Q. (2012): Control principle and technology of final compression ratio of backfilling materials. *Journal of Mining & Safety Engineering*, vol. 29, no. 3, pp. 351-356.

Zhou, Y. J.; Guo, H. Z.; Cao, Z. Z.; Zhang, J. G. (2013): Mechanism and control of water seepage of vertical feeding borehole for solid materials in backfilling coal mining. *International Journal of Mining Science and Technology*, vol. 23, no. 5, pp. 675-679.

Zhou, Z. G.; Tian, S.; Zhang, J. W. (2016): Effects of stacking sequence and impactor diameter on impact damage of glass fiber reinforced aluminum alloy laminate. *CMC: Computers Materials & Continua*, vol. 52, no. 2, pp. 105-121.